5.74 Introductory Quantum Mechanics II
Spring 2009

## 10.3. <u>THIRD-ORDER NONLINEAR SPECTROSCOPIES</u>

Third-order nonlinear spectroscopies are the most widely used class of nonlinear methods, including the common pump-probe experiment. This section will discuss a number of these methods. The approach here is meant to be practical, with the emphasis on trying to connect the particular signals with their microscopic origin. This approach can be used for describing any experiment in terms of the wave-vector, frequency and time-ordering of the input fields, and the frequency and wavevector of the signal.

Selecting signals by wavevector

The question that arises is how to select particular contributions to the signal. Generally, it will not be possible to uniquely select particular diagrams. However you can use the properties of the incident and detected fields to help with selectivity. Here is a strategy for describing a particular experiment:

1) Start with the wavevector and frequency of the signal field of interest.
2) (a) Time-domain: Define a time-ordering along the incident wavevectors or

   (b) Frequency domain: Define the frequencies along the incident wavevectors.
3) Sum up diagrams for correlation functions that will scatter into the wave-vector matched direction, keeping only resonant terms (rotating wave approximation). In the frequency domain, use ladder diagrams to determine which correlation functions yield signals that pass through your filter/monochromator.

Let's start by discussing how one can distinguish a rephasing signal from a non-rephasing signal. Consider two degenerate third-order experiments ($\omega_1 = \omega_2 = \omega_3 = \omega_{sig}$) which are distinguished by the signal wave-vector for a particular time-ordering. We choose a box geometry, where the three incident fields (*a,b,c*) are crossed in the sample, incident from three corners of the box, as shown. (Note that the color in these figures is not meant to represent the frequency of the incident fields –which are all the

$$k_{sig} = +k_a - k_b + k_c$$
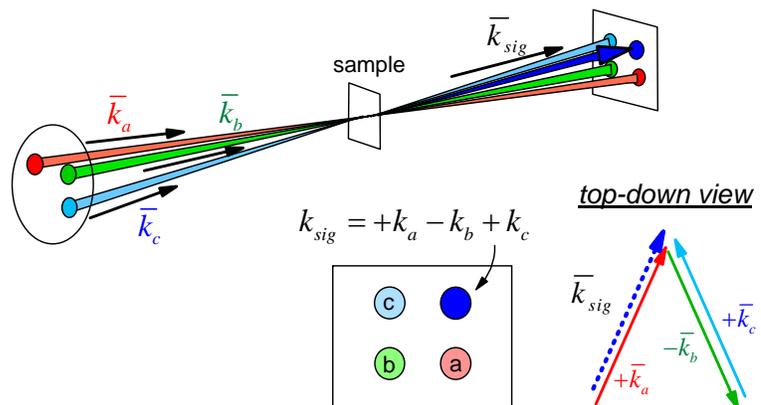
same – but rather is just there to distinguish them for the picture). Since the frequencies are the same, the length of the wavevector $|k| = 2\pi n/\lambda$ is equal for each field, only its direction varies. Vector addition of the contributing terms from the incident fields indicates that the signal $\bar{k}_{sig} = +\bar{k}_a - \bar{k}_b + \bar{k}_c$ will be radiated in the direction of the last corner of the box when observed after the sample. (The colors in the figure do not represent frequency, but just serve to distinguish the beams).

Now, comparing the wavevector matching condition for this signal with those predicted by the third-order Feynman diagrams, we see that we can select non-rephasing signals R_1 and R_4 by setting the time ordering of pulses such that $a = 1$, $b = 2$, and $c = 3$. The rephasing signals R_2 and R_3 are selected with the time-ordering $a = 2$, $b = 1$, and $c = 3$.

Alternatively, we can recognize that both signals can be observed by simultaneously detecting signals in two different directions. If we set the time ordering to be $a = 1$, $b = 2$, and $c = 3$, then the rephasing and non-rephasing signals will be radiated as shown below:

$$\bar{k}_{sig}^R = -\bar{k}_1 + \bar{k}_2 + \bar{k}_3 \qquad \bar{k}_{sig}^{NR} = +\bar{k}_1 - \bar{k}_2 + \bar{k}_3$$
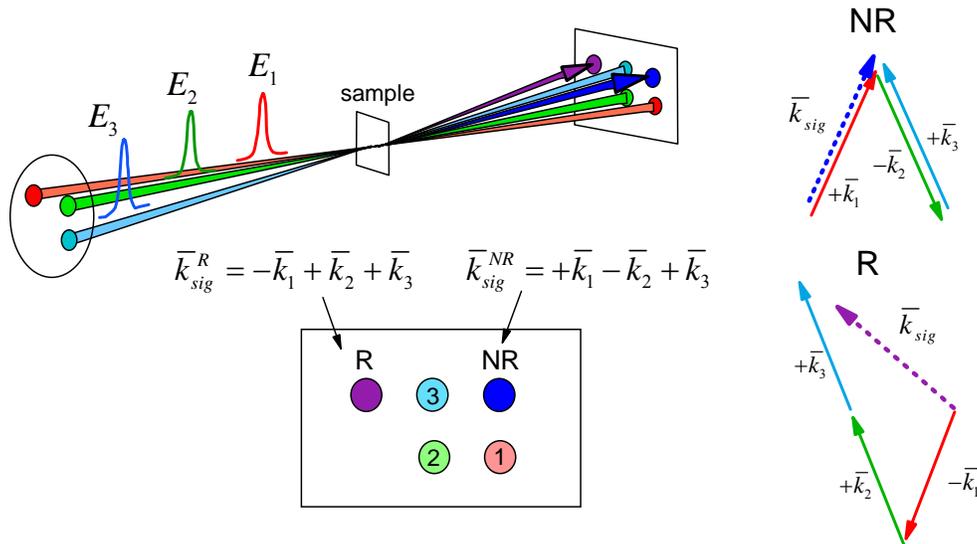
In this case the wave-vector matching for the rephasing signal is imperfect. The vector sum of the incident fields $\bar{k}_{sig}$ dictates the direction of propagation of the radiated signal (momentum conservation), whereas the magnitude of the signal wavevector $\bar{k}'_{sig}$ is dictated by the radiated frequency (energy conservation). The efficiency of radiating the signal field falls of with the wave-vector mismatch $\Delta k = \bar{k}_{sig} - \bar{k}'_{sig}$, as $\left| \bar{E}_{sig}(t) \right| \propto \bar{P}(t) \text{sinc}(\Delta k l/2)$ where l is the path length (see eq. 1.10).

Photon Echo

The photon echo experiment is most commonly used to distinguish static and dynamic line-broadening, and time-scales for energy gap fluctuations. The rephasing character of R_2 and R_3 allows you to separate homogeneous and inhomogeneous broadening. To demonstrate this let's describe a photon echo experiment for an inhomogeneous lineshape, that is a convolution of a homogeneous line shape with width Γ with a static inhomogeneous distribution of width Δ. Remember that linear spectroscopy cannot distinguish the two:
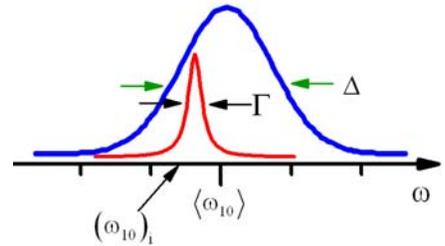
$$R(\tau)=\left|\mu_{ab}\right|^2 e^{-i\omega_{ab}\tau-g(\tau)}-c.c. \tag{10.1}$$

For an inhomogeneous distribution, we could average the homogeneous response, $g(t)=\Gamma_{ba}t$, with an inhomogeneous distribution

$$R=\int d\omega_{ab}\,G(\omega_{ab})R(\omega_{ab}) \tag{10.2}$$

which we take to be Gaussian

$$G(\omega_{ba})=\exp\left(-\frac{\left(\omega_{ba}-\left\langle\omega_{ba}\right\rangle\right)^2}{2\Delta^2}\right). \tag{10.3}$$

Equivalently, since a convolution in the frequency domain is a product in the time domain, we can set

$$g(t)=\Gamma_{ba}t+\tfrac{1}{2}\Delta^2\,t^2. \tag{10.4}$$

So for the case that $\Delta>\Gamma$, the absorption spectrum is a broad Gaussian lineshape centered at the mean frequency $\left\langle\omega_{ba}\right\rangle$ which just reflects the static distribution Δ rather than the dynamics in Γ.

Now look at the experiment in which two pulses are crossed to generate a signal in the direction

$$k_{sig}=2k_2-k_1 \tag{10.5}$$

This signal is a special case of the signal $(k_3+k_2-k_1)$ where the second and third interactions are both derived from the same beam. Both non-rephasing diagrams contribute here, but since both second and third interactions are coincident, $\tau_2=0$ and $R_2=R_3$. The nonlinear signal can be obtained by integrating the homogeneous response,

Two-pulse photon echo
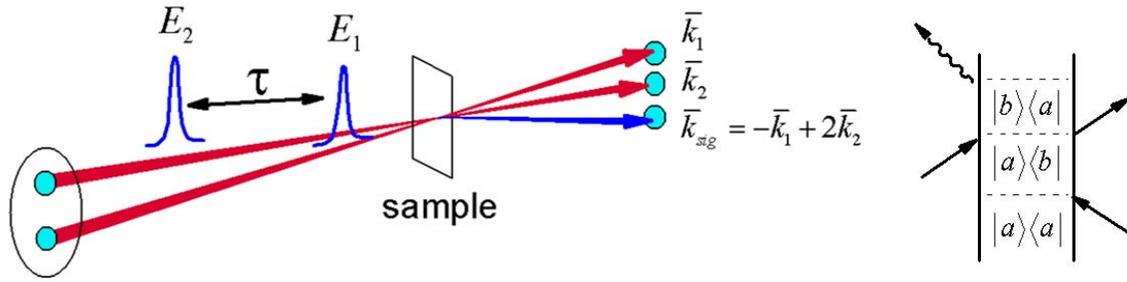
$$R^{(3)}(\omega_{ab}) = |\mu_{ab}|^4 \, p_a \, e^{-i\omega_{ab}(\tau_1-\tau_3)} e^{-\Gamma_{ab}(\tau_1+\tau_3)} \qquad (10.6)$$

over the inhomogeneous distribution as in eq. (10.2). This leads to

$$R^{(3)} = |\mu_{ab}|^4 \, p_a \, e^{-i\langle\omega_{ab}\rangle(\tau_1-\tau_3)} \, e^{-\Gamma_{ab}(\tau_1+\tau_3)} \, e^{-(\tau_1-\tau_3)^2\Delta^2/2} \qquad (10.7)$$

For $\Delta \gg \Gamma_{ab}$, $R^{(3)}$ is sharply peaked at $\tau_1 = \tau_3$, i.e. $e^{-(\tau_1-\tau_3)^2\Delta^2/2} \approx \delta(\tau_1-\tau_3)$. The broad distribution of frequencies rapidly dephases during τ_1, but is rephased (or refocused) during τ_3, leading to a large constructive enhancement of the polarization at $\tau_1=\tau_3$. This rephasing enhancement is called an echo.
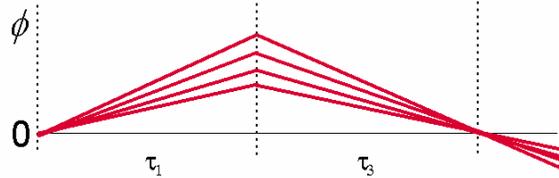
In practice, the signal is observed with a integrating intensity-level detector placed into the signal scattering direction. For a given pulse separation τ (setting $\tau_1=\tau$), we calculated the integrated signal intensity radiated from the sample during τ_3 as

$$I_{sig}(\tau) = |E_{sig}|^2 \propto \int_{-\infty}^{\infty} d\tau_3 \left| P^{(3)}(\tau,\tau_3) \right|^2 \qquad (10.8)$$

In the inhomogeneous limit ($\Delta \gg \Gamma_{ab}$), we find

$$I_{sig}(\tau) \propto |\mu_{ab}|^8 \, e^{-4\Gamma_{ab}\tau} . \qquad (10.9)$$

In this case, the only source of relaxation of the polarization amplitude at $\tau_1 = \tau_3$ is Γ_{ab}. At this point inhomogeneity is removed and only the homogeneous dephasing is measured. The factor of four in the decay rate reflects the fact that damping of the initial coherence evolves over two periods $\tau_1 + \tau_3 = 2\tau$, and that an intensity level measurement doubles the decay rate of the polarization.

Transient Grating

The transient grating is a third-order technique used for characterizing numerous relaxation processes, but is uniquely suited for looking at optical excitations with well-defined spatial period. The first two pulses are set time-coincident, so you cannot distinguish which field interacts first. Therefore, the signal will have contributions both from $k_{sig} = k_1 - k_2 + k_3$ and $k_{sig} = -k_1 + k_2 + k_3$. That is the signal depends on $R_1+R_2+R_3+R_4$.
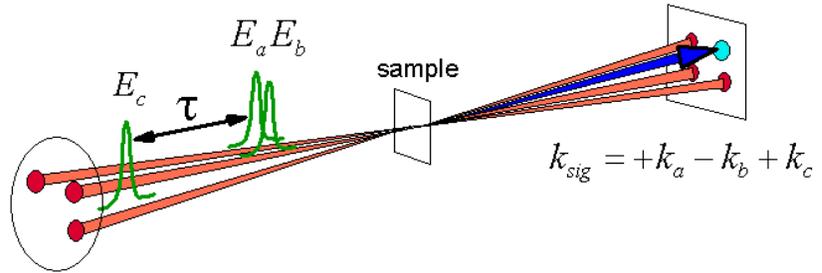
Consider the terms contributing to the polarization that arise from the first two interactions. For two time-coincident pulses of the same frequency, the first two fields have an excitation profile in the sample

$$\bar{E}_a \bar{E}_b = E_a E_b \exp\left[-i\left(\omega_a - \omega_b\right)t + i\left(\bar{k}_a - \bar{k}_b\right)\cdot\bar{r}\right] + c.c. \tag{10.10}$$
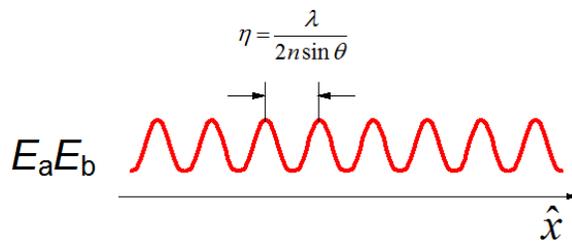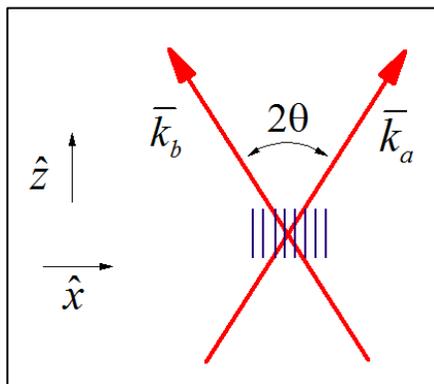
If the beams are crossed at an angle 2θ

$$\begin{aligned}
\bar{k}_a &= |k_a|\left(\hat{z}\cos\theta + \hat{x}\sin\theta\right) \\
\bar{k}_b &= |k_b|\left(\hat{z}\cos\theta - \hat{x}\sin\theta\right)
\end{aligned} \tag{10.11}$$

with

$$|k_a| = |k_b| = \frac{2\pi n}{\lambda}, \tag{10.12}$$

the excitation of the sample is a spatial varying interference pattern along the transverse direction

$$\bar{E}_a\,\bar{E}_b = E_a\,E_b\,\exp\!\left[i\,\bar{\beta}\cdot\bar{x}\right]+c.c. \tag{10.13}$$

The grating wavevector is

$$\bar{\beta}=\bar{k}_1-\bar{k}_2$$
$$\left|\bar{\beta}\right|=\frac{4\pi n}{\lambda}\sin\theta=\frac{2\pi}{\eta}. \tag{10.14}$$

This spatially varying field pattern is called a grating, and has a fringe spacing

$$\eta=\frac{\lambda}{2n\sin\theta}. \tag{10.15}$$

Absorption images this pattern into the sample, creating a spatial pattern of excited and ground state molecules. A time-delayed probe beam can scatter off this grating, where the wavevector matching conditions are equivalent to the constructive interference of scattered waves at the Bragg angle off a diffraction grating. For $\omega_1=\omega_2=\omega_3=\omega_{sig}$ this the diffraction condition is incidence of $\bar{k}_3$ at an angle θ, leading to scattering of a signal out of the sample at an angle $-\theta$. Most commonly, we measure the intensity of the scattered light, as given in eq. (10.8).

More generally, we should think of excitation with this pulse pair leading to a periodic spatial variation of the complex index of refraction of the medium. Absorption can create an excited state grating, whereas subsequent relaxation can lead to heating a periodic temperature profile (a thermal grating). Nonresonant scattering processes (Raleigh and Brillouin scattering) can create a spatial modulation in the real index or refraction. Thus, the transient grating signal will be sensitive to any processes which act to wash out the spatial modulation of the grating pattern:
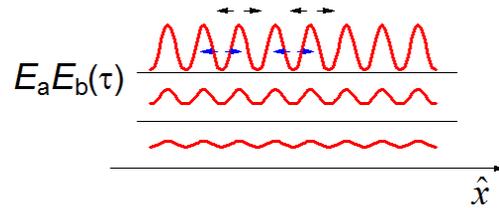
- Population relaxation leads to a decrease in the grating amplitude, observed as a decrease in diffraction efficiency.

$$I_{sig}\left(\tau\right)\propto\exp\!\left[-2\Gamma_{bb}\tau\right] \tag{10.16}$$
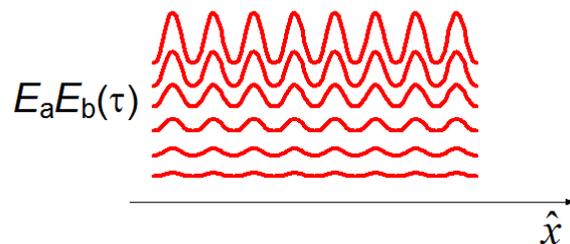
- Thermal or mass diffusion along $\hat{x}$ acts to wash out the fringe pattern. For a diffusion constant D the decay of diffraction efficiency is

$$I_{sig}(\tau) \propto \exp\left[-2\beta^2 D\tau\right] \qquad (10.17)$$


- Rapid heating by the excitation pulses can launch counter propagating acoustic waves along $\hat{x}$, which can modulate the diffracted beam at a frequency dictated by the period for which sound propagates over the fringe spacing in the sample.
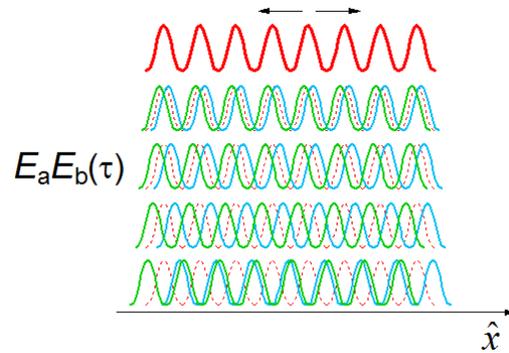
Pump-Probe

The pump-probe or transient absorption experiment is perhaps the most widely used third-order nonlinear experiment. It can be used to follow many types of time-dependent relaxation processes and chemical dynamics, and is most commonly used to follow population relaxation, chemical kinetics, or wavepacket dynamics and quantum beats.

The principle is quite simple, and the using the theoretical formalism of nonlinear spectroscopy often unnecessary to interpret the experiment. Two pulses separated by a delay τ are crossed in a sample: a pump pulse and a time-delayed probe pulse. The pump pulse E_{pu} creates a non-equilibrium state, and the time-dependent changes in the sample are characterized by the probe-pulse E_{pr} through the pump-induced intensity change on the transmitted probe, ΔI.
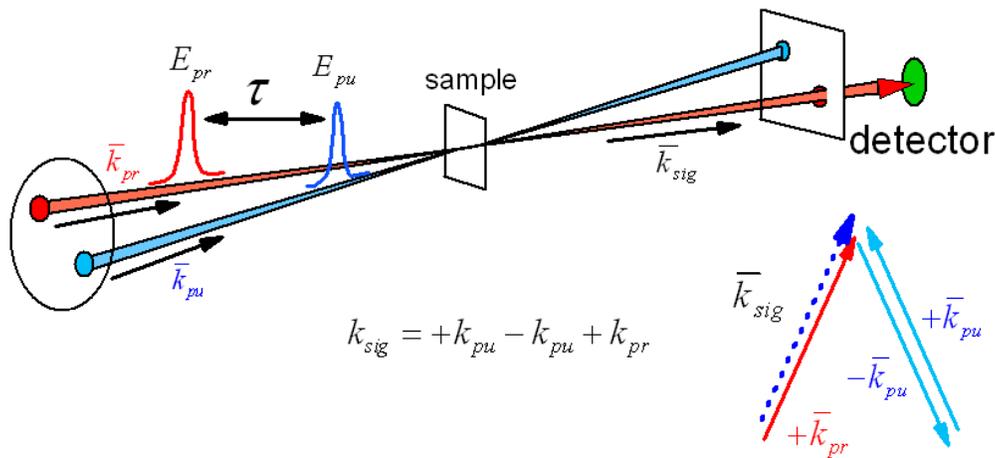
Described as a third-order coherent nonlinear spectroscopy, the signal is radiated collinear to the transmitted probe field, so the wavevector matching condition is $\bar{k}_{sig} = +\bar{k}_{pu} - \bar{k}_{pu} + \bar{k}_{pr} = \bar{k}_{pr}$. There are two interactions with the pump field and the third interaction is with the probe. Similar to the transient grating, the time-ordering of pump-interactions cannot be distinguished, so terms that contribute to scattering along the probe are $k_{sig} = \pm k_1 \mp k_2 + k_3$, i.e. all correlation functions R_1 to R_4. In fact, the pump-probe can be thought of as the limit of the transient grating experiment in the limit of zero grating wavevector (θ and $\beta \rightarrow 0$).

The detector observes the intensity of the transmitted probe and nonlinear signal

$$I = \frac{nc}{4\pi} \left| E'_{pr} + E_{sig} \right|^2 . \tag{10.18}$$

E'_{pr} is the transmitted probe field corrected for linear propagation through the sample. The measured signal is typically the differential intensity on the probe field with and without the pump field present:

$$\Delta I(\tau) = \frac{nc}{4\pi}\left\{\left|E'_{pr} + E_{sig}(\tau)\right|^2 - \left|E'_{pr}\right|^2\right\}.$$ (10.19)

If we work under conditions of a weak signal relative to the transmitted probe $\left|E'_{pr}\right| \gg \left|E_{sig}\right|$, then the differential intensity in eq. (10.19) is dominated by the cross term

$$\Delta I(\tau) \approx \frac{nc}{4\pi}\left[E'_{pr}E^*_{sig}(\tau) + c.c.\right]$$
$$= \frac{nc}{2\pi}\mathrm{Re}\left[E'_{pr}E^*_{sig}(\tau)\right]$$ (10.20)

So the pump-probe signal is directly proportional to the nonlinear response. Since the signal field is related to the nonlinear polarization through a $\pi/2$ phase shift,

$$\overline{E}_{sig}(\tau) = i\frac{2\pi\omega_{sig}\ell}{nc}P^{(3)}(\tau).$$ (10.21)

the measured pump-probe signal is proportional to the imaginary part of the polarization

$$\Delta I(\tau) = 2\omega_{sig}\ell\,\mathrm{Im}\left[E'_{pr}P^{(3)}(\tau)\right],$$ (10.22)

which is also proportional to the correlation functions derived from the resonant diagrams we considered earlier.

Dichroic and Birefringent Response

In analogy to what we observed earlier for linear spectroscopy, the nonlinear changes in absorption of the transmitted probe field are related to the imaginary part of the susceptibility, or the imaginary part of the index of refraction. In addition to the fully resonant processes, it is also possible for the pump field to induce nonresonant changes to the polarization that modulate the real part of the index of refraction. These can be described through a variety of nonresonant interactions, such as nonresonant Raman, the optical Kerr effect, coherent Raleigh or Brillouin scattering, or the second hyperpolarizability of the sample. In this case, we can describe the time-development of the polarization and radiated signal field as

$$P^{(3)}(\tau,\tau_3) = P^{(3)}(\tau,\tau_3)e^{-i\omega_{sig}\tau_3} + \left[P^{(3)}(\tau,\tau_3)\right]^* e^{i\omega_{sig}\tau_3}$$
$$= 2\,\mathrm{Re}\left[P^{(3)}(\tau,\tau_3)\right]\cos(\omega_{sig}\tau_3) + 2\,\mathrm{Im}\left[P^{(3)}(\tau,\tau_3)\right]\sin(\omega_{sig}\tau_3)$$ (10.23)

$$\bar{E}_{sig}(\tau_3) = \frac{4\pi\omega_{sig}\ell}{nc}\left(\text{Re}\left[P^{(3)}(\tau,\tau_3)\right]\sin(\omega_{sig}\tau_3) + \text{Im}\left[P^{(3)}(\tau,\tau_3)\right]\cos(\omega_{sig}\tau_3)\right)$$

$$= E_{bir}(\tau,\tau_3)\sin(\omega_{sig}\tau_3) + E_{dic}(\tau,\tau_3)\cos(\omega_{sig}\tau_3) \tag{10.24}$$

Here the signal is expressed as a sum of two contributions, referred to as the birefringent (E_{bir}) and dichroic (E_{dic}) responses. As before the imaginary part, or dichroic response, describes the sample-induced amplitude variation in the signal field, whereas the birefringent response corresponds to the real part of the nonlinear polarization and represents the phase-shift or retardance of the signal field induced by the sample.

In this scheme, the transmitted probe is

$$\bar{E}'_{pr}(\tau_3) = E'_{pr}(\tau_3)\cos(\omega_{pr}\tau_3), \tag{10.25}$$

So that the

$$\Delta I(\tau) \approx \frac{nc}{2\pi}\left[E'_{pr}(\tau)E_{dic}(\tau)\right] \tag{10.26}$$

Because the signal is in-quadrature with the polarization ($\pi/2$ phase shift), the absorptive or dichroic response is in-phase with the transmitted probe, whereas the birefringent part is not observed. If we allow for the phase of the probe field to be controlled, for instance through a quarter-wave plate before the sample, then we can write

$$\bar{E}'_{pr}(\tau_3,\varphi) = E'_{pr}(\tau_3)\cos(\omega_{pr}\tau_3 + \varphi), \tag{10.27}$$

$$I(\tau,\varphi) \approx \frac{nc}{2\pi}\left[E'_{pr}(\tau)E_{bir}(\tau)\sin(\varphi) + E'_{pr}(\tau)E_{dic}(\tau)\cos(\varphi)\right] \tag{10.28}$$

The birefringent and dichroic response of the molecular system can now be observed for phases of $\phi = \pi/2, 3\pi/2\dots$ and $\phi = 0, \pi\dots$, respectively.

Incoherent pump-probe experiments

What information does the pump-probe experiment contain? Since the time delay we control is the second time interval τ_2, the diagrams for a two level system indicate that these measure population relaxation:

$$\Delta I(\tau) \propto |\mu_{ab}|^4 e^{-\Gamma_{bb}\tau} \tag{10.29}$$

In fact measuring population changes and relaxation are the most common use of this experiment. When dephasing is very rapid, the pump-probe can be interpreted as an incoherent

experiment, and the differential intensity (or absorption) change is proportional to the change of population of the states observed by the probe field. The pump-induced population changes in the probe states can be described by rate equations that describe the population relaxation, redistribution, or chemical kinetics.

For the case where the pump and probe frequencies are the same, the signal decays as a results of population relaxation of the initially excited state. The two-level system diagrams indicate that the evolution in τ_2 is differentiated by evolution in the ground or excited state. These diagrams reflect the equal signal contributions from the ground state bleach (loss of ground state population) and stimulated emission from the excited state. For direct relaxation from excited to ground state the loss of population in the excited state Γ_{bb} is the same as the refilling of the hole in the ground state Γ_{aa}, so that $\Gamma_{aa} = \Gamma_{bb}$. If population relaxation from the excited state is through an intermediate, then the pump-probe decay will reflect equal contributions from both processes, which can be described by coupled first-order rate equations.

When the resonance frequencies of the pump and probe fields are different, then the incoherent pump-probe signal is related to the joint probability of exciting the system at ω_{pu} and detecting at ω_{pr} after waiting a time τ, $P\left(\omega_{pr}, \tau; \omega_{pu}\right)$.

Coherent pump-probe experiments

Ultrafast pump-probe measurements on the time-scale of vibrational dephasing operate in a coherent regime where wavepackets prepared by the pump-pulse modulate the probe intensity. This provides a mechanism for studying the dynamics of excited electronic states with coupled vibrations and photoinitiated chemical reaction dynamics. If we consider the case of pump-probe experiments on electronic states where $\omega_{pu} = \omega_{pr}$, our description of the pump-probe from Feynmann diagrams indicates that the pump-pulse creates excitations both on the excited state and ground state. Both wavepackets will contribute to the signal.
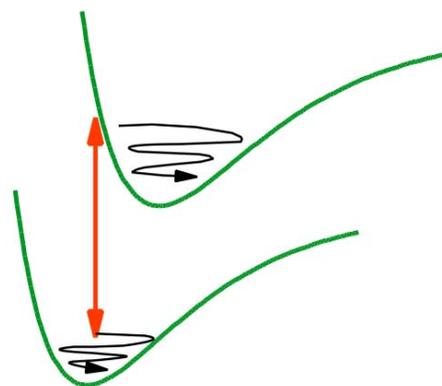
There are two equivalent ways of describing the experiment, which mirror our earlier description of electronic spectroscopy for an electronic transition coupled to nuclear motion.

The first is to describe the spectroscopy in terms of the eigenstates of H_0, $|e, n\rangle$. The second draws on the energy gap Hamiltonian to describe the spectroscopy as two electronic levels H_S that interact with the vibrational degrees of freedom H_B, and the wavepacket dynamics are captured by H_{SB}.

For the eigenstate description, a two level system is inadequate to capture the wavepacket dynamics. Instead, describe the spectroscopy in terms of the four-level system diagrams given earlier. In addition to the population relaxation terms, we see that the R_2 and R_4 terms describe the evolution of coherences in the excited electronic state, whereas the R_1 and R_3 terms describe the ground state wave packet. For an underdamped wavepacket these coherences are observed as quantum beats on the pump-probe signal.
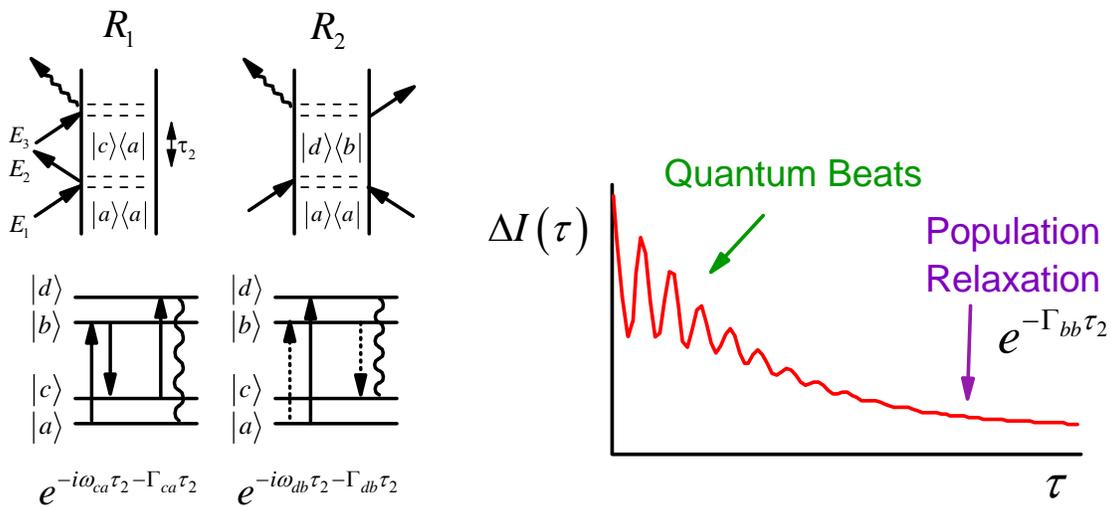
CARS (Coherent Anti-Stokes Raman Scattering)

Used to drive ground state vibrations with optical pulses or cw fields.

- Two fields, with a frequency difference equal to a vibrational transition energy, are used to excite the vibration.
- The first field is the "pump" and the second is the "Stokes" field.
- A second interaction with the pump frequency lead to a signal that radiates at the anti-Stokes frequency: $\omega_{sig} = 2\omega_P - \omega_S$ and the signal is observed background-free next to the transmitted pump field: $\bar{k}_{sig} = 2\bar{k}_P - \bar{k}_S$.
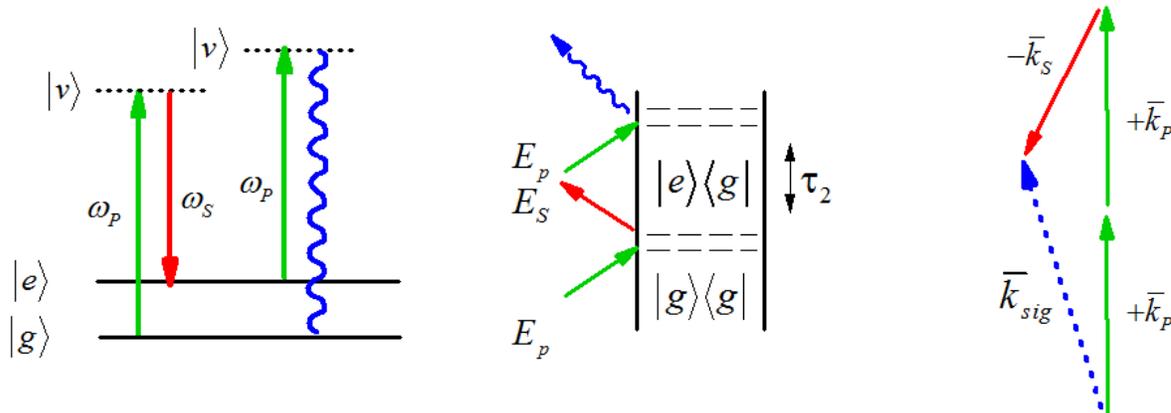
The experiment is described by R_1 to R_4, and the polarization is

$$R^{(3)} = \bar{\mu}_{ev'}\bar{\mu}_{v'g}\ e^{-i\omega_{eg}\tau - \Gamma_{eg}\tau}\bar{\mu}_{gv}\bar{\mu}_{ve} + c.c.$$
$$= \bar{\alpha}_{eg}\,e^{-i\omega_{eg}\tau - \Gamma_{eg}\tau}\bar{\alpha}_{ge} + c.c.$$

The CARS experiment is similar to a linear experiment in which the lineshape is determined by the Fourier transform of $C(\tau) = \langle \bar{\alpha}(\tau)\bar{\alpha}(0) \rangle$.

The same processes contribute to Optical Kerr Effect Experiments and Impulsive Stimulated Raman Scattering.